Carbonates in the Martian meteorite Allan Hills 84001 formed at 18 ± 4 °C in a near-surface aqueous environment

Itay Halevy[1,2], Woodward W. Fischer, and John M. Eiler

Geological and Planetary Sciences, California Institute of Technology, 1200 East California Boulevard, Pasadena, CA 91125

Edited by Mark H. Thiemens, University of California San Diego, La Jolla, CA, and approved September 2, 2011 (received for review June 10, 2011)

Despite evidence for liquid water at the surface of Mars during the Noachian epoch, the temperature of early aqueous environments has been impossible to establish, raising questions of whether the surface of Mars was ever warmer than today. We address this problem by determining the precipitation temperature of secondary carbonate minerals preserved in the oldest known sample of Mars' crust—the approximately 4.1 billion-year-old meteorite Allan Hills 84001 (ALH84001). The formation environment of these carbonates, which are constrained to be slightly younger than the crystallization age of the rock (i.e., 3.9 to 4.0 billion years), has been poorly understood, hindering insight into the hydrologic and carbon cycles of earliest Mars. Using "clumped" isotope thermometry we find that the carbonates in ALH84001 precipitated at a temperature of approximately 18 °C, with water and carbon dioxide derived from the ancient Martian atmosphere. Furthermore, covarying carbonate carbon and oxygen isotope ratios are constrained to have formed at constant, low temperatures, pointing to deposition from a gradually evaporating, subsurface water body—likely a shallow aquifer (meters to tens of meters below the surface). Despite the mild temperatures, the apparently ephemeral nature of water in this environment leaves open the question of its habitability.

The extreme difficulty in achieving mild surface temperatures in early Mars climate models (1) is in disagreement with widespread geomorphological evidence for surface water runoff during the Noachian epoch (2, 3). A robust determination of the temperature at or near the surface of Noachian Mars would provide insight into this apparent paradox, but has been challenging to establish. Carbonate minerals can record and preserve information regarding the temperature and chemistry of their formation environment through aspects of their oxygen and carbon isotopic composition ($\delta^{18}O$ and $\delta^{13}C$, respectively). These minerals have been observed in a range of Martian geological materials, including dust, bedrock outcrops, and several meteorites (4–9). Collectively, these observations highlight a role for carbonate formation in the global Martian carbon cycle and the evolution of its atmosphere. The oldest known carbonate from Mars, or any other planetary body, occurs as a minor constituent (approximately 1% by weight) in the meteorite Allan Hills 84001 (ALH84001), which has a crystallization age of approximately 4.1 billion years (10). The carbonate in ALH84001, geochronologically constrained to be slightly younger in age [between 3.9 and 4.0 billion years old; (11)], provides a unique window into the hydrologic cycle, carbon cycle, and climate of Noachian Mars.

Texturally, the carbonates in ALH84001 occur as (*i*) chemically and isotopically zoned ovoid concretions, veins, and void fillings and (*ii*) regions of massive carbonate, variably intergrown with unweathered feldspathic glass and orthopyroxene, the latter of which makes up the bulk of the meteorite (12–14). The concretions display wide systematic variation in chemical and isotopic composition. They have Ca-Fe-rich cores with $\delta^{18}O_{SMOW}$ (O isotope ratios reported relative to Standard Mean Ocean Water) values as low as approximately 5‰ and $\delta^{13}C_{PDB}$ (C isotope ratios reported relative to the Pee Dee Belemnite standard) values of 25–35‰ (15–18). Their rims are Mg-rich, sometimes nearly pure $MgCO_3$, and have $\delta^{18}O_{SMOW}$ and $\delta^{13}C_{PDB}$ values as high as approximately 30‰ and 65‰, respectively. The veins and void fillings display covarying chemical and isotopic compositions similar to the concretions (12). The massive carbonates are usually internally homogeneous, though chemical and isotopic variability has been observed between isolated occurrences. Several studies have reported an ankeritic (Ca-rich) and isotopically light ($\delta^{18}O_{SMOW}$ of 0–10‰) composition for the massive carbonates (e.g., ref. 16).

The carbonates in ALH84001 have been studied by a variety of geochemical and petrographic methods, but no agreement exists concerning the processes and environment of their precipitation. Hypotheses for their formation span a range of temperatures between subfreezing and more than 700 °C, a range of depths between the surface and several kilometers, and a range of processes including impact melting of preexisting carbonates, hydrothermal alteration of crustal rocks, precipitation from a rapidly evaporating water body, and biological activity (13–16, 19–28). Textural observations indicate that after carbonate growth, ALH84001 experienced brief, localized, shock-related heating, but natural remanent magnetization and argon thermochronometry place upper limits of approximately 40 °C on the short-duration (approximately 10 min) and approximately 20–30 °C on the long-duration (billions of years) thermal history of this rock (29, 30).

Previous methods for estimating the temperature of carbonate formation in ALH84001, though informative, have placed only loose constraints (e.g., refs. 29 and 30) or have depended on assumptions about the chemical and isotopic composition of the carbonate's parent fluid (e.g., refs. 16 and 22). Multiply substituted, or "clumped," isotope thermometry avoids this problem because it is based on homogeneous thermodynamic equilibrium within the carbonate mineral (31, 32). The abundance of rare isotopologues, measured as mass 47 CO_2 (mostly $^{13}C^{18}O^{16}O$) evolved from acid digestion of carbonate minerals, is higher than predicted from a random distribution of the heavy isotopes. This excess is denoted Δ_{47} and varies systematically with carbonate precipitation temperature (32, 33). With temperature known, measurements of the $\delta^{18}O$ and $\delta^{13}C$ of the carbonates provide direct constraints on the isotopic compositions of their parent fluid (water and CO_2).

Author contributions: I.H. and J.M.E. designed research; I.H. performed research; I.H. contributed new reagents/analytic tools; I.H., W.W.F., and J.M.E. analyzed data; and I.H., W.W.F., and J.M.E. wrote the paper.

The authors declare no conflict of interest.

This article is a PNAS Direct Submission.

[1]To whom correspondence may be addressed at: Environmental Sciences and Energy Research, Weizmann Institute of Science, Rehovot, 76100, Israel. E-mail: Itay.Halevy@Weizmann.ac.il.

[2]Present address: Weizmann Institute of Science, Rehovot, 76100, Israel.

This article contains supporting information online at www.pnas.org/lookup/suppl/doi:10.1073/pnas.1109444108/-/DCSupplemental.

Table 1. Isotopic composition of ALH84001 carbonates extracted by stepped acid digestion

	0–1 h					1–4 h					4–12 h				
	N	δ^{18}O‰	δ^{13}C‰	Δ_{47}‰	*T* °C	*N*	δ^{18}O‰	δ^{13}C‰	Δ_{47}‰	*T* °C	*N*	δ^{18}O‰	δ^{13}C‰	Δ_{47}‰	*T* °C
Aliquot A (320 mg)	—	13.05	35.52	—	—	—	16.68	40.87	—	—	—	18.96	40.82	—	—
Aliquot B (1,625 mg)	5	13.38 (±0.28)	34.60 (±0.07)	0.642 (±0.039)	27 $(^{+13}_{-11})$	5	17.32 (±0.28)	41.05 (±0.07)	0.638 (±0.039)	28 $(^{+13}_{-11})$	1	17.99 (±0.28)	40.94 (±0.07)	0.742 (±0.098)	3 $(^{+25}_{-19})$
Aliquot C (1,550 mg)	8	14.11 (±0.16)	35.14 (±0.02)	0.693 (±0.027)	14 $(^{+7}_{-6})$	9	16.27 (±0.16)	40.67 (±0.02)	0.643 (±0.027)	26 $(^{+8}_{-7})$	7	18.17 (±0.16)	42.39 (±0.02)	0.711 (±0.028)	10 $(^{+7}_{-6})$

δ^{18}O and δ^{13}C are reported relative to the SMOW and PDB standards, respectively. *N* is the number of data acquisitions suitable for clumped isotope analysis (typical clumped isotope measurements comprise eight acquisitions), reflecting the gas yield from the digestion steps. Error estimates are based on identical treatment of carbonate standards of known bulk and clumped isotopic composition, which was only done for aliquots B and C (*SI Text*)

Results

We performed stepped phosphoric acid digestions of three aliquots of ALH84001 and measured the bulk and clumped isotopic composition of the evolved CO_2 (see *Methods* and *SI Text*). The amount of CO_2 evolved from the digestion steps was about one-tenth to one-third the amount typically required for clumped isotope analysis. Additionally, the acid digestion duration was up to 36 times longer than typically applied, increasing the potential for contamination. This combination of factors necessitated special extraction apparatus, purification steps, and analytical protocols (*SI Text*, Table S1, and Figs. S1–S3). The δ^{18}O and δ^{13}C values of the carbonate extracted in the three digestion steps (Table 1 and Table S2) were reproducible among the three different meteorite aliquots and fall within the range of previous measurements (15–18, 21, 22). Combining these δ^{18}O and δ^{13}C measurements with prior constraints on the relationship between stable isotope and major element composition in ALH84001 carbonates (15–18), we estimated the chemical composition of carbonate sampled by the digestion steps (Fig. 1 and *SI Text*). The sequential extraction technique yielded increasing Mg content with reaction time, a relationship expected from the slower dissolution of the Mg-rich outer concretion layers (34).

The first aliquot of the meteorite (approximately 320 mg) yielded too little gas for reliable Δ_{47} measurements, but has δ^{18}O and δ^{13}C values that are consistent with subsequent extractions of two larger aliquots (1,625 and 1,550 mg, respectively). The Δ_{47} measurements of these two larger aliquots (Table 1) yield six temperatures between 3^{+25}_{-19} and 30^{+13}_{-11} °C, all within uncertainty of an error-weighted average temperature of 18 ± 4 °C.

Discussion

Establishing the Robustness of the Temperature Determination. We addressed potential sources of uncertainty (outside of analytical uncertainty) in interpreting the Δ_{47} data as a precipitation temperature for the carbonates in ALH84001. The crystal orientation distribution of the carbonate concretions (*SI Text* and Fig. S4) suggests that the carbonates have not been subject to recrystallization since their radial growth from aqueous solution. In the absence of recrystallization, resetting of the carbonates' isotopic composition to yield the observed, strongly covarying relationship between δ^{18}O and δ^{13}C is unlikely. Together, these observations indicate that the measured Δ_{47} was acquired during initial carbonate precipitation.

Precipitation at high temperature and subsequent reordering of carbonate clumped isotopes upon cooling is unlikely because the temperature recorded under such a scenario (i.e., blocking temperature) would be approximately 200–300 °C (35, 36). Mixing between two physical or isotopic end members with bulk isotopic composition at either end of the observed δ^{13}C and δ^{18}O range in ALH84001 carbonate may lead to spuriously low apparent temperatures, but is also unlikely, as indicated both by previous observations of the distribution of ALH84001 carbonate chemical and isotopic composition (15–18) and by limits on the time scale for isotopic equilibrium (*SI Text* and Fig. S5).

Several additional hypotheses for interpreting the Δ_{47} data can be rejected on the basis of the relationships observed among the δ^{18}O, δ^{13}C, and Δ_{47} measured in the carbonate (Fig. 2). Carbonate precipitation over a range of temperatures (e.g., ref. 22) does not fit the observed δ^{18}O and δ^{13}C array (Fig. 2*A*). Because the stepped acid digestion could not perfectly separate the concretion cores from their rims, the range of $\delta^{18}O_{SMOW}$ we observed was narrow (approximately 13–19‰) relative to the full range observed in microprobe studies (approximately 5–30‰). As a result, the uncertainty in a linear fit to the reliable δ^{18}O-Δ_{47} data (aliquots B and C) is large at the ends of the full δ^{18}O range (Fig. 2*B*, dashed curves). Thus, in a formal hypothesis testing sense, the 95% confidence bounds marginally include an explanation of the data by kinetic isotope effects (KIEs) of the sort observed in some cave and cryogenic carbonates (37–40). These KIEs, which are thought to arise in part from rapid, disequilibrium CO_2 degassing, have been observed to lead to spurious apparent values of Δ_{47} that are lower than the true values by as much as 0.12‰. Applied to our measured Δ_{47}, this would translate into an error-weighted average temperature of carbonate formation in ALH84001 of −7 °C (instead of approximately 18 °C if the Δ_{47} we measure is correct). Temperatures below 0 °C can be rejected because they would cause the water from which the carbonates formed to freeze and are thus inconsistent with the increase in δ^{18}O from the concretion cores to their rims. The remaining temperature range between 0 and 18 °C is possible, but the large uncertainty in the fit and the better correspondence to a hypothesis of constant temperature (Fig. 2*B*) lead us to conclude that KIEs of the type discussed above are unlikely in

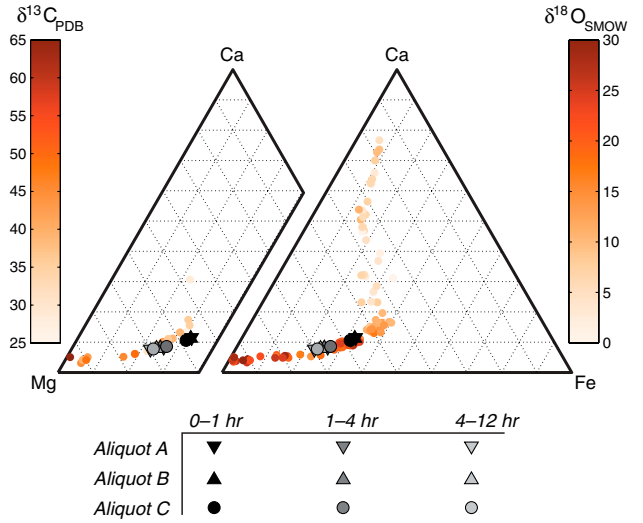

Fig. 1. Major element composition of the ALH84001 carbonates digested in the three steps, estimated from their δ^{18}O and δ^{13}C values and correlations between major element and isotopic composition (see text).

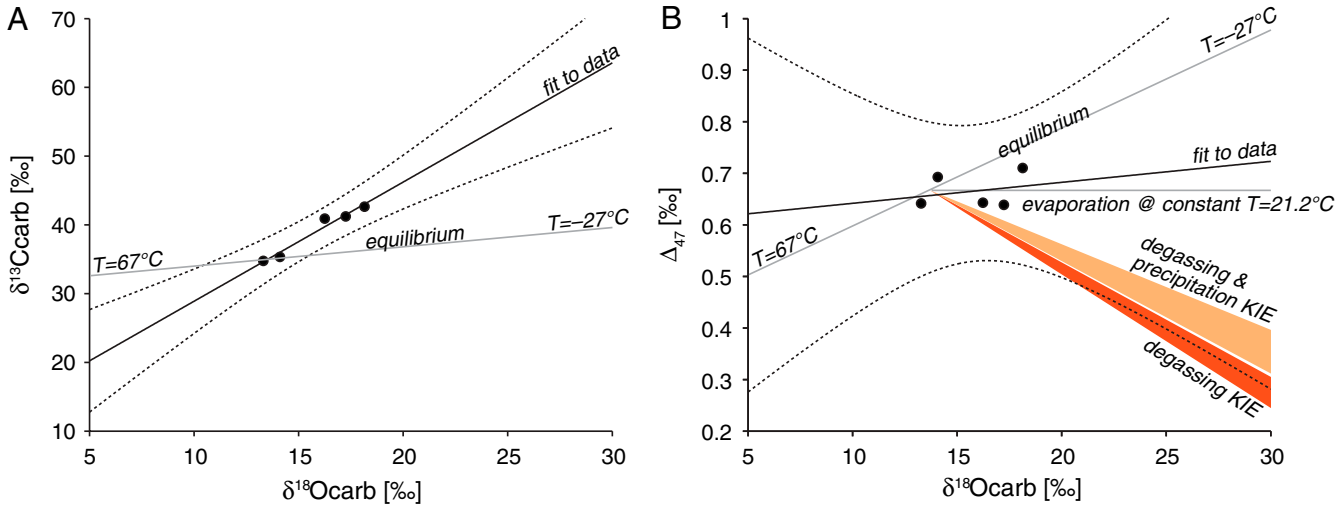

Fig. 2. Comparison of Δ_{47}, $\delta^{18}O$, and $\delta^{13}C$ values (see *SI Text*) with models for the isotopic variation in ALH84001 carbonates. (*A*) Relationship between $\delta^{13}C$ and $\delta^{18}O$. The solid black line and the broken black curves are a weighted total least squares linear fit to the data and a 95% confidence bound on the fit, respectively. The diagonal gray line shows the equilibrium relationship between $\delta^{13}C$ and $\delta^{18}O$ over the range of temperatures required to explain the range of $\delta^{18}O_{SMOW}$ observed in microprobe studies (approximately 5–30‰). A hypothesis of evolving temperature can be rejected on the basis of the misfit between these lines. (*B*) Relationship between Δ_{47} and $\delta^{18}O$. The solid black line and the broken black curves are a weighted total least squares linear fit to the data and a 95% confidence bound on the fit, respectively. The diagonal gray line shows the equilibrium relationship between Δ_{47} and $\delta^{18}O$ over the range of temperatures required to explain the observed $\delta^{18}O_{SMOW}$ range (approximately 5–30‰). The horizontal gray line shows the isotopic evolution due to evaporation at a constant temperature. The temperature of 21.2 °C is the average temperature of the two leftmost data points. The light and dark orange wedges are model predictions for the relationship between Δ_{47} and $\delta^{18}O$ that is expected from rapid degassing and associated kinetic isotope effects (38). The confidence bounds on the fit to the data are most consistent with constant temperature, less consistent with an evolving temperature (which can be ruled out by the relationship between $\delta^{13}C$ and $\delta^{18}O$) and only marginally include kinetic isotope effects due to rapid degassing (see text).

the case of ALH84001 carbonates. Altogether the data are best explained by carbonate precipitation at a constant temperature of approximately 18 °C. This result rules out a high-temperature origin of ALH84001 carbonates (e.g., refs. 13, 14, and 19) and imposes strict constraints on the remaining low-temperature hypotheses.

Formation Environment of ALH84001 Carbonates. Previously only loose constraints on the temperature of carbonate growth in ALH84001 were available, and past models for their formation required one or more assumptions about temperature, the open/closed nature of the system, the ratio of CO_2 to H_2O, or the isotopic composition of the parent fluid. Here, by independently constraining temperature, we are able to use the isotopic variation in the carbonates to develop a model for their formation environment and mechanism.

From the Δ_{47} constraints, we find that the striking core to rim coevolution of $\delta^{18}O_{SMOW}$ (approximately $5 \rightarrow 30‰$) and $\delta^{13}C_{PDB}$ (approximately $25 \rightarrow 65‰$), observed in previous ion-microprobe studies (15–18) is best explained by gradual evaporation of a shallow subsurface aqueous solution at a constant, low temperature. The evaporative water loss drives carbonate precipitation and CO_2 degassing under equilibrium conditions. The observed isotopic variation in the carbonates suggests a system in poor short-term communication with the atmosphere—otherwise the $\delta^{18}O$ and $\delta^{13}C$ would be buffered by exchange with the atmospheric CO_2 reservoir. This rules out, for example, formation of the ALH84001 carbonates in a long-lasting, open lake. Instead we suggest that distillative loss of the isotopically light vapor phase (gaseous CO_2 and water vapor) from a semiisolated environment (Fig. 3*A*) gradually enriched the residual water and dissolved inorganic carbon in the heavy isotopes, resulting in the coupled increase in $\delta^{18}O$ and $\delta^{13}C$ values from the concretion cores to their rims. A system open to the atmosphere, where evaporation and carbonate precipitation occurred too rapidly to allow equilibrium with the gas phase, may also be consistent with the

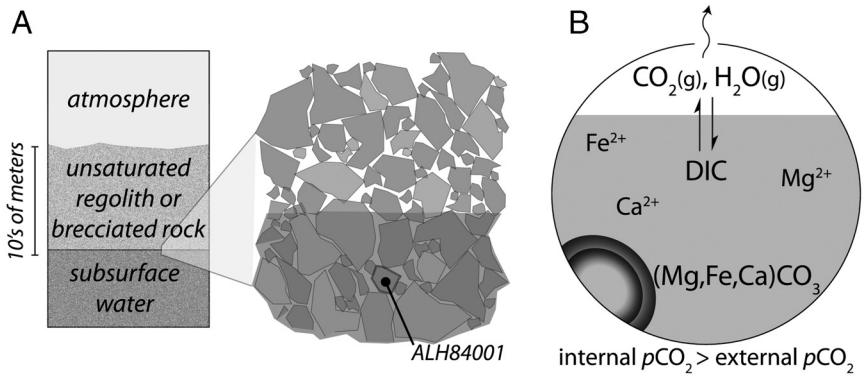

Fig. 3. Model for carbonate formation in ALH84001. (*A*) Physical model of a shallow subsurface aquifer. The depth of carbonate formation is constrained by a combination of the cosmic ray exposure pattern of ALH84001 and Martian meteorite ejection models (48, 49). (*B*) Reduction of the physical model to a geochemical model of carbonate precipitation and CO_2 degassing driven by gradual evaporation of water in a confined volume, coupled to loss of the vapor phase.

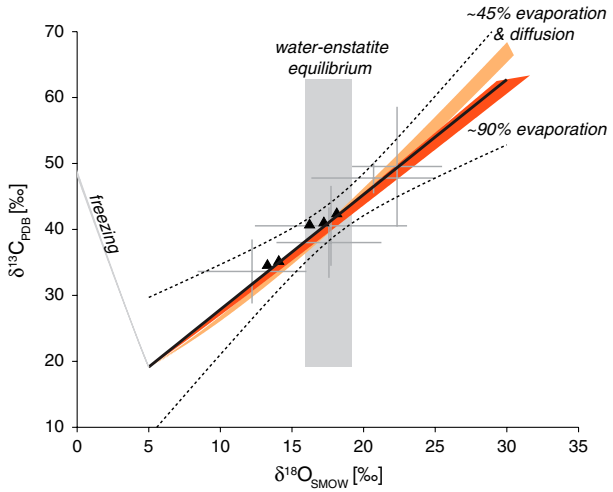

Fig. 4. Comparison of observed and modeled isotopic composition. Gray crosses are combinations of $\delta^{18}O$ and $\delta^{13}C$ microprobe data correlated by Mg content, including uncertainty in the correlation (*SI Text*). The black curves show a weighted total least squares linear fit through these data (solid) and 95% confidence bounds on the fit (broken). The black triangles are measurements from this study. The gray rectangle brackets the highest values of $\delta^{18}O_{SMOW}$ achievable by water–rock oxygen isotope exchange, given the uncertainty on temperature and on the measured $\delta^{18}O$ of the ALH84001 silicates (*SI Text*). The light orange field shows the coevolution of $\delta^{18}O$ and $\delta^{13}C$ during 42% evaporation and diffusion-limited water loss from a subsurface reservoir, accompanied by carbonate precipitation and CO_2 degassing and diffusion, at a temperature of 17.5 ± 5 °C (*SI Text*). The darker orange field is for 92% evaporative water loss and accompanying carbonate precipitation if transport to the surface is not rate-limited by diffusion. The gray line with a negative slope shows the $\delta^{18}O$ and $\delta^{13}C$ coevolution if the water slowly freezes instead of evaporating. The initial pCO_2 in the calculations was 600 millibar and the nonprecipitating solute concentrations were 0 mol liter^{-1}. The results are relatively insensitive to this choice (*SI Text* and Fig. S6).

coevolution of $\delta^{18}O$ and $\delta^{13}C$ values, but is not supported by the observed $\delta^{18}O$-Δ_{47} relationship (Fig. 2*B*). Finally, although the observed $\delta^{13}C$ increase can also be explained by organic matter synthesis or oxidation, the existence of extraterrestrial organic matter in ALH84001 remains controversial, due mainly to the difficulty in ruling out contamination by terrestrial organic matter (27). Furthermore, the covariation in carbon and oxygen isotope ratios suggests a common process affected both reservoirs.

Support for the hypothesis of carbonate formation from an evaporating subsurface aqueous reservoir comes from observed covariation between $\delta^{18}O$ and $\delta^{13}C$ in terrestrial carbonates from cold or arid regions. These analogs are imperfect because even in cold, dry, and relatively organic-poor environments, organic matter fixation or respiration contributes to the preserved isotopic signal to variable degree. Even so, the isotopic composition of Mg-bearing carbonates formed on ultramafic mine tailings in northwestern Canada (latitude ≥58 °N) form arrays strikingly similar to those observed in ALH84001 carbonates in $\delta^{18}O$-$\delta^{13}C$ space (41), as do endostromatolites in an impact structure in the Canadian high Arctic (42), soil carbonates from the Mojave and Atacama deserts (43, 44), and caliche formed on basalts in young volcanic fields in Arizona (45). All of these studies discuss hypotheses that explain the observed isotopic trends with evaporation and CO_2 degassing.

To further examine this hypothesis we developed a model of carbonate precipitation (Fig. 3*B*) in which carbonate mineral saturation and charge balance are maintained, as is chemical and isotopic equilibrium among the aqueous solution, the instantaneous precipitate, and the gas phase in the regolith during gradual evaporation (*Methods* and *SI Text*). The range of $\delta^{18}O$ values in the concretions requires distillative loss of 42–92% of the water, depending on whether the transport of water toward the surface is rate limited by vapor-phase diffusion. The observed covariation in $\delta^{18}O$ and $\delta^{13}C$ can be reproduced (Fig. 4) if approximately 87–98% of the noncarbonate carbon loss from solution is transported to the surface. The remaining 2–13% causes a pore pCO_2 increase of 5–15%, consistent with the modest pressure gradient that would be required to cause distillative CO_2 loss from the subsurface in the scenario considered here. These results are relatively insensitive to the choice of initial pCO_2, the nonprecipitating ion concentration, and the particular carbonate mineralogy (*SI Text* and Fig. S6).

Although the fluid in an environment such as the one we describe could, in principle, come from depth (magmatic or hydrothermal fluid), there is evidence that the parent fluid of the ALH84001 carbonates came from the surface (atmosphere–hydrosphere). The carbonates have an oxygen isotopic composition that is anomalous with respect to Martian igneous rocks [$\Delta^{17}O > 0.3$; (46)]. Similarly, sulfides in this sample have a "mass-independent" sulfur isotopic composition [$\Delta^{33}S \neq 0$; (47)]. Both signatures were likely generated by atmospheric reactions and support a surface source of the fluid. Furthermore, water in oxygen isotope equilibrium with the Ca-rich concretion cores (determined by microprobe studies) would, at the temperatures we measured, have $\delta^{18}O$ more than 10‰ lower than equilibrium with coexisting silicate minerals (Fig. S7) and CO_2 in equilibrium with the concretion cores is tens of *permil* too high in $\delta^{13}C$ to have come directly from the Martian mantle (though the $\delta^{13}C$ of the Martian mantle is poorly constrained, *SI Text*).

At the measured growth temperature, the Mg-rich carbonates in the concretion rims have $\delta^{18}O$ 10–15‰ heavier than equilibrium with the silicates (Fig. S7). This, together with the persistence of the mass-anomalous oxygen isotope composition, implies that the combination of time and temperature was insufficient to allow appreciable oxygen isotope exchange between water and rock, supporting a low-temperature, transient aqueous environment. This is consistent also with the absence of alteration minerals (e.g., hydrous phyllosilicates) in ALH84001 other than the carbonates and the associated sulfides and magnetite (13, 14).

Conclusions

In sum, the evidence points to a short-lived, low-temperature, aqueous environment, initially containing surface-derived CO_2 and H_2O but subsequently characterized by poor communication with the atmosphere, such that isotopic buffering did not occur. Distillative loss of CO_2 and H_2O can explain the observed $\delta^{18}O$ and $\delta^{13}C$ trends. This combination of characteristics is consistent with partial to complete evaporation of a subsurface aqueous reservoir, coupled to carbonate precipitation and CO_2 degassing under equilibrium conditions. We imagine that an ephemeral regolith aquifer at a depth of a few to tens of meters would be a plausible setting for this process (Fig. 3). The existence of a near-surface aqueous environment during the Noachian epoch, recorded by the carbonates in ALH84001, is consistent with, though need not require, a warmer early Mars—a hydrothermal or impact-related source for the required heat is equally possible. Though the mild temperatures point to an environment that might be considered habitable, the presence of water was also ephemeral, suggesting a time frame probably too short for life to have evolved de novo.

Methods

Three aliquots of ALH84001 were subjected to stepped phosphoric acid digestion. Because of the slower dissolution kinetics of magnesian carbonates, the first step in each of the digestions (0–1 h) sampled the faster-reacting, Ca-rich carbonates, whereas the second and third steps (1–4 and 4–12 h, respectively) sampled more Mg-rich compositions (34). Finer separation (e.g., by lower reaction temperature or shorter reaction intervals) was not attempted due to the relatively large amount of CO_2 required for clumped isotope analysis, the susceptibility of small samples to contamina-

tion, and the precious nature of the sample. The bulk and clumped isotopic composition of evolved CO_2 was measured on a Thermo Finnigan MAT 253 isotope ratio gas source mass spectrometer. The small sample size necessitated measurement using a microvolume. Measurements were standardized to carbonates of known bulk and clumped isotopic composition, treated identically to the meteorite aliquots and measured using a microvolume. See *SI Text* for full analytical methods.

With knowledge of the precipitation temperature, we constructed an isotopic evolution model and examined hypotheses for carbonate precipitation that could also quantitatively explain the observed covariation of carbon and oxygen isotope ratios in the carbonate. Prescribing values for the model-free parameters—the initial CO_2 pressure (pCO_2) and the concentration of non-precipitating ions—we solve for the pH, solute concentrations, and pCO_2 as the water evaporates. The oxygen isotopic evolution depends on the cumulative fraction of water lost to evaporation and vapor-phase diffusion. The carbon removed by carbonate precipitation is equal to the loss of the precipitating cation, which is solved by the model. The remaining carbon lost from solution is divided between transport to the surface and an increase in pore pCO_2. The carbon isotopic evolution, therefore, depends on the relative proportions of these removal processes (carbonate precipitation, diffusive transport, and pore overpressurization). See *SI Text* for a full description of the model and parametric sensitivity analysis results.

ACKNOWLEDGMENTS. We thank N. Kitchen for assistance with the isotopic analyses. We thank two anonymous reviewers for valuable comments that have improved this work. I.H. was funded by a Texaco Postdoctoral Fellowship (Division of Geological and Planetary Sciences, Caltech). J.M.E. acknowledges funding from National Aeronautics and Space Administration and National Science Foundation-Division of Earth Sciences.

1. Haberle RM (1998) Early Mars climate models. *J Geophys Res* 103:28467–28479.
2. Carr MH (1996) *Water on Mars* (Oxford Univ Press, New York) p vii.
3. Fassett CI, Head JW (2008) Valley network-fed, open-basin lakes on Mars: Distribution and implications for Noachian surface and subsurface hydrology. *Icarus* 198:37–56.
4. Bandfield JL, Glotch TD, Christensen PR (2003) Spectroscopic identification of carbonate minerals in the martian dust. *Science* 301(5636):1084–1087.
5. Boynton WV, et al. (2009) Evidence for calcium carbonate at the Mars Phoenix Landing Site. *Science* 325:61–64.
6. Ehlmann BL, et al. (2008) Orbital identification of carbonate-bearing rocks on Mars. *Science* 322:1828–1832.
7. Michalski JR, Niles PB (2010) Deep crustal carbonate rocks exposed by meteor impact on Mars. *Nat Geosci* 3:751–755.
8. Morris RV, et al. (2010) Identification of carbonate-rich outcrops on Mars by the Spirit Rover. *Science* 329:421–424.
9. Grady MM, Wright I (2006) The carbon cycle on early Earth—and on Mars? *Philos Trans R Soc Lond B Biol Sci* 361:1703–1713.
10. Lapen TJ, et al. (2010) A younger age for ALH84001 and its geochemical link to shergottite sources in Mars. *Science* 328(5976):347–351.
11. Borg LE, et al. (1999) The age of the carbonates in martian meteorite ALH84001. *Science* 286:90–94.
12. Corrigan CM, Harvey RP (2004) Multi-generational carbonate assemblages in martian meteorite Allan Hills 84001: Implications for nucleation, growth, and alteration. *Meteorit Planet Sci* 39:17–30.
13. Mittlefehldt DW (1994) ALH84001, a cumulate orthopyroxenite member of the Martian meteorite clan. *Meteoritics* 29:214–221.
14. Treiman AH (1995) A petrographic history of Martian meteorite ALH84001: 2 shocks and an ancient age. *Meteoritics* 30:294–302.
15. Leshin LA, McKeegan KD, Carpenter PK, Harvey RP (1998) Oxygen isotopic constraints on the genesis of carbonates from Martian meteorite ALH84001. *Geochim Cosmochim Acta* 62:3–13.
16. Eiler JM, Valley JW, Graham CM, Fournelle J (2002) Two populations of carbonate in ALH84001: Geochemical evidence for discrimination and genesis. *Geochim Cosmochim Acta* 66:1285–1303.
17. Saxton JM, Lyon IC, Turner G (1998) Correlated chemical and isotopic zoning in carbonates in the Martian meteorite ALH84001. *Earth Planet Sci Lett* 160:811–822.
18. Niles PB, Leshin LA, Guan Y (2005) Microscale carbon isotope variability in ALH84001 carbonates and a discussion of possible formation environments. *Geochim Cosmochim Acta* 69:2931–2944.
19. Scott ERD, Yamaguchi A, Krot AN (1997) Petrological evidence for shock melting of carbonates in the Martian meteorite ALH84001. *Nature* 387:377–379.
20. Harvey RP, McSween HY (1996) A possible high-temperature origin for the carbonates in the Martian meteorite ALH84001. *Nature* 382:49–51.
21. Valley JW, et al. (1997) Low-temperature carbonate concretions in the Martian meteorite ALH84001: Evidence from stable isotopes and mineralogy. *Science* 275:1633–1638.
22. Romanek CS, et al. (1994) Record of fluid-rock interactions on Mars from the meteorite ALH84001. *Nature* 372:655–657.
23. Warren PH (1998) Petrologic evidence for low-temperature, possibly flood evaporitic origin of carbonates in the ALH84001 meteorite. *J Geophys Res* 103:16759–16773.
24. McSween HY, Harvey RP (1998) An evaporation model for formation of carbonates in the ALH84001 Martian meteorite. *Int Geol Rev* 40:774–783.
25. Eiler JM, Kitchen N, Leshin L, Strausberg M (2002) Hosts of hydrogen in Allan Hills 84001: Evidence for hydrous martian salts in the oldest martian meteorite? *Meteorit Planet Sci* 37:395–405.
26. McKay DS, et al. (1996) Search for past life on Mars: Possible relic biogenic activity in Martian meteorite ALH84001. *Science* 273:924–930.
27. Jull AJT, Courtney C, Jeffrey DA, Beck JW (1998) Isotopic evidence for a terrestrial source of organic compounds found in martian meteorites Allan Hills 84001 and Elephant Moraine 79001. *Science* 279:366–369.
28. Golden DC, et al. (2001) A simple inorganic process for formation of carbonates, magnetite, and sulfides in Martian meteorite ALH84001. *Am Mineral* 86:370–375.
29. Weiss BP, et al. (2000) A low temperature transfer of ALH84001 from Mars to Earth. *Science* 290:791–795.
30. Cassata WS, Shuster DL, Renne PR, Weiss BP (2010) Evidence for shock heating and constraints on Martian surface temperatures revealed by 40Ar/39Ar thermochronometry of Martian meteorites. *Geochim Cosmochim Acta* 74:6900–6920.
31. Eiler JM, Schauble E (2004) $^{18}O^{13}C^{16}O$ in Earth's atmosphere. *Geochim Cosmochim Acta* 68:4767–4777.
32. Ghosh P, et al. (2006) ^{13}C-^{18}O bonds in carbonate minerals: A new kind of paleothermometer. *Geochim Cosmochim Acta* 70:1439–1456.
33. Huntington KW, et al. (2009) Methods and limitations of 'clumped' CO_2 isotope (Δ_{47}) analysis by gas-source isotope ratio mass spectrometry. *J Mass Spectrom* 44:1318–1329.
34. Al-Aasm IS, Taylor BE, South B (1990) Stable isotope analysis of multiple carbonate samples using selective acid extraction. *Chem Geol* 80:119–125.
35. Eiler JM, Bonifacie M, Daeron M (2009) 'Clumped isotope' thermometry for high-temperature problems. *Geochim Cosmochim Acta* 73:A322.
36. Dennis KJ, Schrag DP (2010) Clumped isotope thermometry of carbonatites as an indicator of diagenetic alteration. *Geochim Cosmochim Acta* 74:4110–4122.
37. Daeron M, et al. (2011) $^{13}C^{18}O$ Clumping in speleothems: Observations from natural caves and precipitation experiments. *Geochim Cosmochim Acta* 75:3303–3317.
38. Guo W (2009) Carbonate clumped isotope thermometry: Application to carbonaceous chondrites and effects of kinetic isotope fractionation. PhD dissertation (California Inst of Technology, Pasadena, CA).
39. Affek HP, Bar-Matthews M, Ayalon A, Matthews A, Eiler JM (2008) Glacial/interglacial temperature variations in Soreq cave speleothems as recorded by 'clumped isotope' thermometry. *Geochim Cosmochim Acta* 72:5351–5360.
40. Affek HP, Guo W, Daeron M, Eiler JM (2008) 'Clumped isotopes' in speleothem carbonate and atmospheric CO_2—Is there a kinetic isotope effect? *Geochim Cosmochim Acta* 72:A6.
41. Wilson SA, et al. (2009) Carbon dioxide fixation within mine wastes of ultramafic-hosted ore deposits: Examples from the Clinton Creek and Cassiar Chrysotile Deposits, Canada. *Econ Geol* 104:95–112.
42. Lacelle D, Pellerin A, Clark ID, Lauriol B, Fortin D (2009) (Micro) morphological, inorganic-organic isotope geochemisty and microbial populations in endostromatolites (cf. fissure calcretes), Haughton impact structure, Devon Island, Canada: The influence of geochemical pathways on the preservation of isotope biomarkers. *Earth Planet Sci Lett* 281:202–214.
43. Quade J, Cerling TE, Bowman JR (1989) Systematic variations in the carbon and oxygen isotopic composition of pedogenic carbonate along elevation transects in the Southern Great-Basin, United-States. *Geol Soc Am Bull* 101:464–475.
44. Quade J, et al. (2007) Soils at the hyperarid margin: The isotopic composition of soil carbonate from the Atacama Desert, Northern Chile. *Geochim Cosmochim Acta* 71:3772–3795.
45. Knauth LP, Brilli M, Klonowski S (2003) Isotope geochemistry of caliche developed on basalt. *Geochim Cosmochim Acta* 67:185–195.
46. Farquhar J, Thiemens MH, Jackson T (1998) Atmosphere-surface interactions on Mars: $\Delta^{17}O$ measurements of carbonate from ALH 84001. *Science* 280:1580–1582.
47. Farquhar J, Savarino J, Jackson TL, Thiemens MH (2000) Evidence of atmospheric sulphur in the martian regolith from sulphur isotopes in meteorites. *Nature* 404:50–52.
48. Fritz J, Artemieva N, Greshake A (2005) Ejection of Martian meteorites. *Meteorit Planet Sci* 40:1393–1411.
49. Warren PH (1994) Lunar and Martian meteorite delivery services. *Icarus* 111:338–363.